XLIII CILAMCE
21–25, November, 2022
FOZ DO IGUAÇU – PR – BRAZIL

A limit analysis approach for plane stress problem

Eric L. B. Cavalcante[1], Luca G. P. V. Lorenzini[2], Eliseu Lucena Neto[2]

[1]*Tribunal de Contas da União*
70042-900 Brasília, DF, Brazil
ericlb@fastmail.net
[2]*Divisão de Engenharia Civil, Instituto Tecnológico de Aeronáutica*
12228-900, São José dos Campos/SP, Brazil
luca.v.lorenzini@gmail.com, eliseu@ita.br

Abstract. A finite element is developed for plane stress problems based on the static theorem of limit analysis. This four-node quadrilateral element satisfies the equilibrium equations and the mechanical boundary conditions on average, and, as such, it is not expected lower bounds on the collapse load from the computed results. Numerical tests are carried out using the von Mises criterion, which is exactly satisfied throughout the element. The nonlinear convex optimization problem posed here is treated as second-order cone programming and solved with a primal-dual interior-point algorithm implemented in the MOSEK optimization package.

Keywords: static theorem, finite element, second-order cone programming, plane stress.

1 Introduction

For perfectly plastic material with associated flow rule, the theory of plasticity allows lower and upper bound predictions of the collapse load by means of the static and kinematic theorems, respectively [1]. Coupling these theorems with the finite-element method gives rise to large-scale constrained optimization problems that can be solved by means of linear or nonlinear programming techniques.

The usefulness of this very powerful procedure was limited initially by the lack of robustness of the algorithms that were available for solving large-scale mathematical programming problems and by the low computational capability. Considerable challenges have been posed and significant progress has been made over the years [2, 3]. Now, efficient predictions of the collapse load can be made and the procedure has become a simpler alternative to elastoplastic finite element approaches, which require the computationally expensive effort of an evolutive analysis that follows the whole history of loading [4].

The static theorem of limit analysis requires stress fields satisfying the equilibrium equations, the mechanical boundary conditions, and the yield criterion everywhere [5]. In this sense, the multinode triangular element proposed by Belytschko and Hodge [6] for plane stress and the three-node triangular element proposed by Lysmer [7] for plane strain give rigorous lower-bound solution for several usual cases. Owing to its simplicity, the latter has become a reference and inspired many other developments [8, 9]. To the best of the authors' knowledge, it is the only three-node triangular element for computing strict lower bounds on the collapse load of plane problems.

The three-node triangular finite element developed by Cavalcante et al. [10] provides linearly varying stress fields that satisfy the equilibrium equations within the element and the mechanical boundary conditions on average. However, the traction continuity across the element interfaces and the yield criterion are nowhere violated. Discrete plane strain and stress problems, described by Mohr-Coulomb and von Mises criteria, respectively, are considered and dealt with as nonlinear convex programming. The optimization problem is formulated as second-order cone programming and solved using a robust interior-point algorithm implemented in MOSEK [11, 12]. The element performance shows that not satisfying the equilibrium equations and the mechanical boundary conditions exactly seems to be irrelevant in view of its accuracy compared with the

benchmark element proposed by Lysmer and with exact or other excellent numerical references found in the literature.

Triangles are quite convenient for mesh generation. However, it is common in two-dimensional finite element modeling that if one has a choice between triangles and quadrilaterals with similar nodal arrangement, preference is given to quadrilaterals. It is in this sense that the numerical procedure of Cavalcante et al. [10] is extend here to incorporate a four-node quadrilateral element with stress bilinearly interpolated. Just as for the triangular element, the quadrilateral element equation is also obtained in explicit form and preliminary investigation of its numerical behavior is provided.

2 Finite Element and Plastic Admissibility

The static approach of the limit analysis requires that the assumed stress field must satisfy the equilibrium equations, the mechanical boundary conditions and the yield criterion everywhere. Under these idealized conditions, the computed limit load is a lower bound on the true collapse load [5].

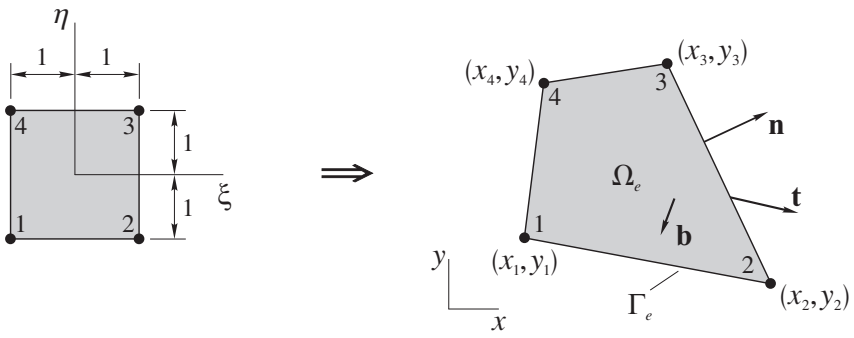

Figure 1. Free-body diagram of the element Ω_e with the unit normal vector $\mathbf{n}$ on its boundary Γ_e, the body force $\mathbf{b}$ and the traction $\mathbf{t}$ activated by the surrounding elements or external agents. The element mapping from the parametric $\xi\eta$ to the Cartesian physical space xy takes place by means of (2).

Suppose that the solid is divided into a number of quadrilateral elements and treated as an assembly of them. An isolated element, sketched on the right of Fig. 1, is a free-body diagram held in equilibrium by the body force $\mathbf{b} = \lfloor b_x \quad b_y \rfloor^T$ and the traction $\mathbf{t} = \lfloor t_x \quad t_y \rfloor^T$ activated by the surrounding elements or external agents. Cavalcante et al. [10] show that the equilibrium equations and the mechanical boundary conditions may be enforced by means of the weak form

$$\int_{\Gamma_u} \mathbf{w}^T \mathbf{t}\, ds + \int_{\Gamma_t} \mathbf{w}^T \bar{\mathbf{t}}\, ds + \int_{\Omega_e} \mathbf{w}^T \mathbf{b}\, dxdy - \int_{\Omega_e} (\mathbf{D}^T \mathbf{w})^T \boldsymbol{\sigma}\, dxdy = 0 \tag{1}$$

where the portion Γ_u and Γ_t of the element boundary Γ_e falls on the solid boundary with prescribed displacement and traction $\bar{\mathbf{t}}$, respectively. The vectors $\mathbf{w} = \lfloor w_x \quad w_y \rfloor^T$ and $\boldsymbol{\sigma} = \lfloor \sigma_x \quad \sigma_y \quad \tau_{xy} \rfloor^T$ represent the weight function and the stress, and $\mathbf{D}$ is a differential operator [10].

Figure 1 shows the element as a square with sides of length 2 defined in local dimensionless coordinates ξ and η which vary from -1 to $+1$, and as a quadrilateral obtained from the square element after a mapping given by

$$x = \sum_{i=1}^{4} N_i x_i \qquad y = \sum_{i=1}^{4} N_i y_i . \tag{2}$$

Any point (x, y) in the quadrilateral (physical element) is given in terms of the nodal coordinates (x_i, y_i) using the interpolation functions

$$N_1 = \frac{1}{4}(1-\xi)(1-\eta) \quad N_2 = \frac{1}{4}(1+\xi)(1-\eta) \quad N_3 = \frac{1}{4}(1+\xi)(1+\eta) \quad N_2 = \frac{1}{4}(1-\xi)(1+\eta). \tag{3}$$

Proceeding in a similar manner, the weight function and stress at any point are interpolated from their nodal values $\mathbf{w}_i$ and $\boldsymbol{\sigma}_i$ by means of

$$\mathbf{w} = \sum_{i=1}^{4} N_i \mathbf{w}_i \qquad \boldsymbol{\sigma} = \sum_{i=1}^{4} N_i \boldsymbol{\sigma}_i . \tag{4}$$

Note that $\mathbf{w}$ and $\boldsymbol{\sigma}$ vary linearly on quadrilateral coordinate lines $\xi =$ constant and $\eta =$ constant, but are not linear polynomials as in the case of the three-node triangle developed by Cavalcante et al. [10].

Substitution of (4) into (1), followed by integration in the parametric space $\xi\eta$, leads to

$$[\mathbf{G}_1 \quad \mathbf{G}_2 \quad \mathbf{G}_3 \quad \mathbf{G}_4] \begin{Bmatrix} \boldsymbol{\sigma}_1 \\ \boldsymbol{\sigma}_2 \\ \boldsymbol{\sigma}_3 \\ \boldsymbol{\sigma}_4 \end{Bmatrix} = \mathbf{F} \tag{5}$$

where

$$\mathbf{G}_1 = \begin{bmatrix} \frac{y_2 - y_4}{6} & 0 & \frac{x_4 - x_2}{6} \\ 0 & \frac{x_4 - x_2}{6} & \frac{y_2 - y_4}{6} \\ \frac{y_3 - 2y_1 + y_4}{12} & 0 & \frac{2x_1 - x_3 - x_4}{12} \\ 0 & \frac{2x_1 - x_3 - x_4}{12} & \frac{y_3 - 2y_1 + y_4}{12} \\ \frac{y_4 - y_2}{12} & 0 & \frac{x_2 - x_4}{12} \\ 0 & \frac{x_2 - x_4}{12} & \frac{y_4 - y_2}{12} \\ \frac{2y_1 - y_2 - y_3}{12} & 0 & \frac{x_2 - 2x_1 + x_3}{12} \\ 0 & \frac{x_2 - 2x_1 + x_3}{12} & \frac{2y_1 - y_2 - y_3}{12} \end{bmatrix}$$

$$\mathbf{G}_2 = \begin{bmatrix} \frac{2y_2 - y_3 - y_4}{12} & 0 & \frac{x_3 - 2x_2 + x_4}{12} \\ 0 & \frac{x_3 - 2x_2 + x_4}{12} & \frac{2y_2 - y_3 - y_4}{12} \\ \frac{y_3 - y_1}{6} & 0 & \frac{x_1 - x_3}{6} \\ 0 & \frac{x_1 - x_3}{6} & \frac{y_3 - y_1}{6} \\ \frac{y_1 - 2y_2 + y_4}{12} & 0 & \frac{2x_2 - x_1 - x_4}{12} \\ 0 & \frac{2x_2 - x_1 - x_4}{12} & \frac{y_1 - 2y_2 + y_4}{12} \\ \frac{y_1 - y_3}{12} & 0 & \frac{x_3 - x_1}{12} \\ 0 & \frac{x_3 - x_1}{12} & \frac{y_1 - y_3}{12} \end{bmatrix}$$

$$\mathbf{G}_3 = \begin{bmatrix} \frac{y_2 - y_4}{12} & 0 & \frac{x_4 - x_2}{12} \\ 0 & \frac{x_4 - x_2}{12} & \frac{y_2 - y_4}{12} \\ \frac{2y_3 - y_1 - y_4}{12} & 0 & \frac{x_1 - 2x_3 + x_4}{12} \\ 0 & \frac{x_1 - 2x_3 + x_4}{12} & \frac{2y_3 - y_1 - y_4}{12} \\ \frac{y_4 - y_2}{6} & 0 & \frac{x_2 - x_4}{6} \\ 0 & \frac{x_2 - x_4}{6} & \frac{y_4 - y_2}{6} \\ \frac{y_1 - 2y_3 + y_2}{12} & 0 & \frac{2x_3 - x_1 - x_2}{12} \\ 0 & \frac{2x_3 - x_1 - x_2}{12} & \frac{y_1 - 2y_3 + y_2}{12} \end{bmatrix}$$

$$\mathbf{G}_4 = \begin{bmatrix} \frac{y_2 - 2y_4 + y_3}{12} & 0 & \frac{2x_4 - x_2 - x_3}{12} \\ 0 & \frac{2x_4 - x_2 - x_3}{12} & \frac{y_2 - 2y_4 + y_3}{12} \\ \frac{y_3 - y_1}{12} & 0 & \frac{x_1 - x_3}{12} \\ 0 & \frac{x_1 - x_3}{12} & \frac{y_3 - y_1}{12} \\ \frac{2y_4 - y_1 - y_2}{12} & 0 & \frac{x_1 - 2x_4 + x_2}{12} \\ 0 & \frac{x_1 - 2x_4 + x_2}{12} & \frac{2y_4 - y_1 - y_2}{12} \\ \frac{y_1 - y_3}{6} & 0 & \frac{x_3 - x_1}{6} \\ 0 & \frac{x_3 - x_1}{6} & \frac{y_1 - y_3}{6} \end{bmatrix}$$

$$\mathbf{F} = \int_{\Gamma_t} [\mathbf{N}_1 \quad \mathbf{N}_2 \quad \mathbf{N}_3 \quad \mathbf{N}_4]^T \bar{\mathbf{t}}\, ds + \int_{\Omega_e} [\mathbf{N}_1 \quad \mathbf{N}_2 \quad \mathbf{N}_3 \quad \mathbf{N}_4]^T \mathbf{b}\, dxdy \tag{6}$$

and

$$\mathbf{N}_i = \begin{bmatrix} N_i & 0 \\ 0 & N_i \end{bmatrix}. \tag{7}$$

Details on how to obtain the element equation (5) in explicit form are given in [13]. Moreover, this reference also proves that the imposition of the von Mises yield criterion $f(\boldsymbol{\sigma}) \leq 0$ at the element nodes implies the satisfaction of the criterion throughout the element. For plane stress,

$$f(\boldsymbol{\sigma}) = \sqrt{\left(\sigma_x - \sigma_y\right)^2 + \sigma_x^2 + \sigma_y^2 + 6\tau_{xy}^2} - \sqrt{2}\sigma_0 \tag{8}$$

where σ_0 is the yield stress in simple tension.

3 Second-Order Cone Programming

In the static approach to limit analysis, the solid equilibrium and the yield criterion, expressed in terms of nodal stresses, are constraints of an optimization problem for the applied load maximization. The optimal solution

$$\lambda^* = \{max\ \lambda \mid \mathbf{L}\bar{\boldsymbol{\sigma}} = \lambda \mathbf{f}_1 + \mathbf{f}_2, \qquad \mathbf{g}(\bar{\boldsymbol{\sigma}}) \leq \mathbf{0}\} \tag{9}$$

identifies the collapse load, where the applied load has been split into two parts: $\lambda\mathbf{f}_1$ which is adjusted during the optimization by means of the load factor λ, and $\mathbf{f}_2$ which is kept constant. The vector $\bar{\boldsymbol{\sigma}}$ collects the nodal stresses.

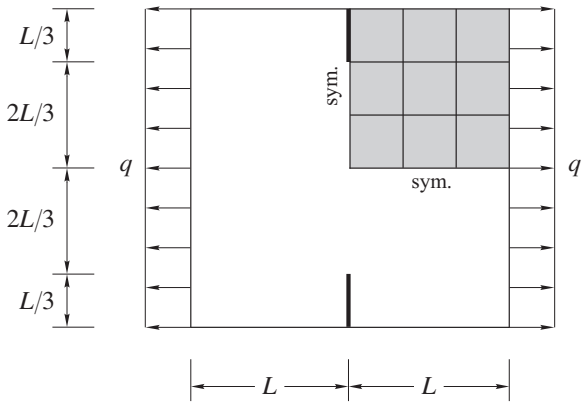

Figure 2. Square plate with symmetric cuts under uniformly distributed load q and solution domain modeled by the 3×3 mesh.

The equality constraint

$$\mathbf{L}\bar{\boldsymbol{\sigma}} = \lambda \mathbf{f}_1 + \mathbf{f}_2, \tag{10}$$

which arises from the assembly of (5), represents the discrete equilibrium of the whole solid. The inequality constraint

$$\mathbf{g}(\bar{\boldsymbol{\sigma}}) \leq \mathbf{0}, \tag{11}$$

which stems from the evaluation at each mesh node of inequality $f(\boldsymbol{\sigma}) \leq 0$, ensures no violation of the yield criterion.

To formulate (9) as a second-order cone programming [14] under the von Mises criterion for plane stress, one introduces the auxiliary variables

$$\mathbf{v} = \begin{Bmatrix} v_1 \\ v_2 \\ v_3 \\ v_4 \end{Bmatrix} = \begin{bmatrix} 1 & -1 & 0 \\ 1 & 0 & 0 \\ 0 & 1 & 0 \\ 0 & 0 & \sqrt{6} \end{bmatrix} \begin{Bmatrix} \sigma_x \\ \sigma_y \\ \tau_{xy} \end{Bmatrix} \tag{12}$$

into the function (8) to state the criterion as the four-dimensional second-order cone

$$\sqrt{v_1^2 + v_2^2 + v_3^2 + v_4^2} \leq \sqrt{2}\sigma_0. \tag{13}$$

Now, the problem (9) can be treated as second-order cone programming by just replacing $\mathbf{g}(\bar{\boldsymbol{\sigma}}) \leq \mathbf{0}$ with

$$\mathbf{g}_1(\bar{\boldsymbol{\sigma}}, \bar{\mathbf{v}}) = \mathbf{0} \qquad \mathbf{g}_2(\bar{\boldsymbol{\sigma}}, \bar{\mathbf{v}}) \leq \mathbf{0}, \tag{14}$$

where the vector $\bar{\mathbf{v}}$ collects the nodal values of $\mathbf{v}$. The new constraints (14) stem from the evaluation of (12) and (13) at each node. Recasting the problem in the form of second-order cone programming is particularly advantageous because it guarantees global convergence and efficiency in the solution process when coupled with a primal-dual interior-point algorithm.

The optimization problem solution is carried out following the steps: (a) set up the problem as second-order cone programming (problem (9) with (11) replaced by (14)) by means of the YALMIP toolbox [15] in the MATLAB [16] environment; (b) solution by MOSEK [12] using the primal-dual interior-point algorithm developed for nonlinear convex optimization by Andersen et al. [11].

4 Numerical Test

The test consists of the square plate of side $2L$, with thin $L/3$ long cuts as shown in Fig. 2, submitted to a uniformly distributed load q acting at two opposite edges. Owing to symmetry consideration, only the right top quarter of the plate is defined as the solution domain subjected to the mechanical boundary conditions: $t_n = t_s =$

0 on the top edge; either $t_n = t_s = 0$ (inside de cut) or $t_s = 0$ (outside de cut) on the left edge; $t_n = q$ and $t_s = 0$ on the right edge; $t_s = 0$ on the bottom edge. The weight function component w_n is made null on the left edge outside the cut and on the bottom edge because t_n is unknown there. Because of the presence of the thin cuts, the stress field is far from homogeneous in this problem.

Table 1 contains the limit load predictions normalized by $q_{\text{ref}} = 1.2744$, which is an excellent collapse load estimate computed by means of the average between the lower and upper bounds obtained by Ciria et al. [8] with $\sigma_0 = \sqrt{3}$. The results obtained with the three-node triangular element [10] are also shown in the table. An $n \times n$ mesh of triangular elements has the same NDV and NC as the respective mesh of quadrilateral elements, but with twice the number of elements. The convergence of q to q_{ref} can be observed as the mesh is refined and this is accomplished monotonically from below. The number of iterations agrees with already published numerical experiments, in the sense that an interior-point method demands typically between 5 and 50 iterations to solve any problem in the form of second-order cone programming problem [14]. The reported CPU_1 times refer to the time spent on the assembly operation and CPU_2 times refer to the time actually spent on the optimization iterations. The computations are performed on a personal laptop computer (Intel Core i7-9750H CPU and 64 GB of RAM) running a 64-bit Windows 10.

Table 1. Collapse load predictions for the plate with symmetric cuts

Mesh	Element	NE	NDV	NC	q/q_{ref}	iter	CPU_1(s)	CPU_2 (s)
3×3	present	9	113	106	0.7268	10	0.53	0.25
	[10]	18			0.7687	10	0.58	0.30
6×6	present	36	344	332	0.8717	10	0.65	0.25
	[10]	72			0.8966	9	0.66	0.28
12×12	present	144	1184	1162	0.9383	12	0.95	0.31
	[10]	288			0.9530	14	0.92	0.39
24×24	present	576	4376	4334	0.9688	15	2.22	0.42
	[10]	1152			0.9765	14	2.17	0.39
48×48	present	2304	16808	16727	0.9835	19	7.30	1.01
	[10]	4608			0.9875	18	7.28	0.95

NE: no. of elements; NDV: no. of design variables; NC: no. of constraints; iter: no. of iterations

5 Conclusions

A numerical procedure is provided for limit analysis of plane strain problems by combining discrete models of four-node quadrilateral finite elements and second-order cone programming. The proposed quadrilateral element has the attractive feature of being explicitly obtained, avoiding the expensive exact integration by four-point Gauss quadrature. An $n \times n$ mesh of triangular elements has the same NDV and NC as the respective mesh of quadrilateral elements, but with twice the number of elements. In this case, the numerical tests show that the predictions of the collapse load are slightly less accurate for the quadrilateral element. As the mesh is refined, the results converge monotonically from below. This, however, demands further detailed examination.

Authorship statement. The authors hereby confirm that they are the sole liable persons responsible for the authorship of this work, and that all material that has been herein included as part of the present paper is either the property (and authorship) of the authors, or has the permission of the owners to be included here.

References

[1] D. C. Drucker, W. Prager and H. J. Greenberg, "Extended limit design theorems for continuous media". *Quarterly of Applied Mathematics*, vol. 9, n. 4, pp. 381–389, 1952.
[2] K. D. Andersen, E. Christiansen, A. R. Conn and M. L. Overton, "An efficient primal-dual interior-point method for minimizing a sum of Euclidean norms". *SIAM Journal on Scientific Computing*, vol. 22, n. 1, pp. 243–262, 2000.
[3] A. Makrodimopoulos and C. M. Martin, "Lower bound limit analysis of cohesive-frictional materials using second-order cone programming". *International Journal for Numerical Methods in Engineering*, vol. 66, n. 4, pp. 604–634, 2006.
[4] E. A. Souza Neto, D. Perić and D. R. J. Owen. *Computational methods for plasticity: theory and applications*. John Wiley, 2008.
[5] W. F. Chen and X. L. Liu. *Limit analysis in soil mechanics*. Elsevier, 1990.
[6] T. Belytschko and P. G. Hodge, "Plane stress limit analysis by finite elements". *Journal of the Engineering Mechanics Division*, vol. 96, n. 6, pp. 931–944, 1970.
[7] J. Lysmer, "Limit analysis of plane problems in soil mechanics". *Journal of the Soil Mechanics and Foundations Division*, vol. 96, n. 4, pp. 1311–1334, 1970.
[8] H. Ciria, J. Peraire and J. Bonet, "Mesh adaptive computation of upper and lower bounds in limit analysis". *International Journal for Numerical Methods in Engineering*, vol. 75, n. 8, pp. 899–944, 2008.
[9] B. Ukritchon and S. Keawsawasvong, "Lower bound limit analysis of an anisotropic undrained strength criterion using second-order cone programming". *International Journal for Numerical and Analytical Methods in Geomechanics*, vol. 42, n. 8, pp. 1016–1033, 2018.
[10] E. L. B.Cavalcante, E. Lucena Neto and D. J. R. Sodré, "A three-node triangular finite element for static limit analysis". *Journal of Engineering Mechanics*, vol. 146, n. 9, pp. 04020099, 2020.
[11] E. D. Andersen, C. Roos and T. Terlaky, "On implementing a primal-dual interior-point method for conic quadratic optimization". *Mathematical Programming*, Series B, vol. 95, n. 2, pp. 249–277, 2003.
[12] MOSEK ApS. *The Mosek Optimization Toolbox for MATLAB Manual*. Version 8.1 (Available from http://docs.mosek.com/8.1/toolbox/index.html) [Accessed in May, 2019].
[13] L. G. P. V. Lorenzini. A Finite Element for Limit Analysis of Plane Stress Problems. MSc thesis (in Portuguese), Instituto Tecnológico de Aeronáutica, 2022.
[14] M. S. Lobo, L. Vandenberghe, S. Boyd and H. Lebret, "Applications of second-order cone programming". *Linear Algebra and its Applications*, vol. 284, n. 1–3, pp. 193–228, 1998.
[15] J. Löfberg, "YALMIP: a toolbox for modeling and optimization in MATLAB". In: IEEE International Symposium on Computer Aided Control System Design, Taipei, pp. 284–289, 2004.
[16] MATLAB. *The MathWorks*. MATLAB, 2018.